OPEN ACCESS

University of BRISTOL

Swim, M., Albertario, A., Iacobazzi, D., Caputo, M., & Ghorbel, M. (2019). Amnion-Based Scaffold with Enhanced Strength and Biocompatibility for In Vivo Vascular Repair. *Tissue Engineering - Part A*, *25*(7-8), 603-619. https://doi.org/10.1089/ten.tea.2018.0175

Peer reviewed version

Link to published version (if available):
10.1089/ten.tea.2018.0175

Link to publication record in Explore Bristol Research
PDF-document

This is the author accepted manuscript (AAM). The final published version (version of record) is available online via Mary Ann Liebert at https://www.liebertpub.com/doi/10.1089/ten.tea.2018.0175 . Please refer to any applicable terms of use of the publisher.

University of Bristol - Explore Bristol Research
General rights

This document is made available in accordance with publisher policies. Please cite only the published version using the reference above. Full terms of use are available:
http://www.bristol.ac.uk/red/research-policy/pure/user-guides/ebr-terms/

For Peer Review

Tissue Engineering

Tissue Engineering Manuscript Central: http://mc.manuscriptcentral.com/ten

Amnion-based scaffold with enhanced strength and biocompatibility for in vivo vascular repair

Journal:	*Tissue Engineering*
Manuscript ID	TEA-2018-0175.R1
Manuscript Type:	Original Article
Date Submitted by the Author:	n/a
Complete List of Authors:	Swim, Megan; University of Bristol, Bristol Medical School Albertario, Ambra; University of Bristol, Bristol Medical School Iacobazzi, Dominga; University of Bristol, Bristol Medical School Caputo, Massimo; University of Bristol, Bristol Medical School Ghorbel, Mohamed; University of Bristol, Bristol Medical School
Keyword:	Blood Vessel < Applications in Tissue Engineering (DO NOT select this phrase; it is a header ONLY), Mesenchymal Stem Cells < Fundamentals of Tissue Engineering (DO NOT select this phrase; it is a header ONLY), Adult Stem Cells < Fundamentals of Tissue Engineering (DO NOT select this phrase; it is a header ONLY), Acellular Biological Matrices < Enabling Technologies in Tissue Engineering (DO NOT select this phrase; it is a header ONLY)
Manuscript Keywords (Search Terms):	Amnion, Decellularization, Tissue Engineering, Mesenchymal Stem Cells, Corrective Heart Surgery
Abstract:	Current vascular replacement grafts used in congenital heart defect corrective surgery have poor longevity and growth potential. Recipient patients often require multiple reoperations. Tissue engineering has the promise to produce a graft with the potential to grow, remodel and repair. Here we aimed at developing an amnion-based scaffold suitable for cardiovascular tissue engineering applications and in vivo usage. The developed human amnion-based scaffold was made by an enzymatic decellularization process followed by freeze-drying as a single or multi-layered structure. These structures were compared to native amnion for seeded cell viability and biomechanical properties then tested for in vivo biocompatibility. Our results demonstrated that while native amnion tissue supported little cell growth, the decellularized-amnion allowed cell engraftment and survival. Additionally, preservation of the scaffold by freeze-drying as a single layer, allowed cell engraftment and growth. Multi-layering the freeze-dried amnion-scaffolds resulted in a similar cell growth potential of the single layered construct but superior mechanical strength. The multi-layered construct showed in vitro biocompatibility with endothelial cells, smooth muscle cells, cardiac myocytes, and thymus and cord-blood-derived MSCs. When implanted in a piglet model of left pulmonary artery grafting, the multi-layered construct showed its in vivo suitability and biocompatibility for vascular repair as demonstrated by the development of newly formed endothelium in the intima, a smooth muscle

	cell-rich medial layer and an adventitia containing new vasa vasorum. In conclusion, our developed amnion-derived scaffold represents an off-the-shelf biocompatible structure that can be seeded with the patient's own MSCs to produce an autologous vascular graft.

SCHOLARONE™
Manuscripts

For Peer Review ONLY// Not for Distribution

Amnion-based scaffold with enhanced strength and biocompatibility for in vivo vascular repair

Megan M Swim, Ambra Albertario, Dominga Iacobazzi, Massimo Caputo[1], Mohamed T Ghorbel[1*]

Bristol Heart Institute, Bristol Medical School, University of Bristol, Research Level 7, Bristol Royal Infirmary, Marlborough Street, BS2 8HW, Bristol, UK.

Additional Footnotes

[1] Co-senior authors.

*Corresponding author (m.ghorbel@bristol.ac.uk)

Running title

Amnion-based scaffold for vascular repair

For Peer Review ONLY/ Not for Distribution

For Peer Review ONLY/Not for Distribution

ABSTRACT

Current vascular replacement grafts used in congenital heart defect corrective surgery have poor longevity and growth potential. Recipient patients often require multiple reoperations. Tissue engineering has the promise to produce a graft with the potential to grow, remodel and repair. Here we aimed at developing an amnion-based scaffold suitable for cardiovascular tissue engineering applications and in vivo usage. The developed human amnion-based scaffold was made by an enzymatic decellularization process followed by freeze-drying as a single or multi-layered structure. These structures were compared to native amnion for seeded cell viability and biomechanical properties then tested for in vivo biocompatibility. Our results demonstrated that while native amnion tissue supported little cell growth, the decellularized-amnion allowed cell engraftment and ~~proliferation cell~~ survival. Additionally, preservation of the scaffold by freeze-drying as a single layer, allowed ~~further improved~~ cell engraftment and ~~cell~~ growth. Multi-layering the freeze-dried amnion-scaffolds resulted in a similar cell growth potential of the single layered construct but superior mechanical strength. The multi-layered construct showed in vitro biocompatibility with endothelial cells, smooth muscle cells, cardiac myocytes, and thymus and cord-blood-derived MSCs. When implanted in a piglet model of left pulmonary artery grafting, the multi-layered construct showed its in vivo suitability and biocompatibility for vascular repair as demonstrated by the development of newly formed endothelium in the intima, a smooth muscle cell-rich medial layer and an adventitia containing new vasa vasorum. ~~endothelial cell layer in the inner side of the graft and a smooth muscle layer in the outer side~~. In conclusion, our developed amnion-derived scaffold represents an off-the-shelf biocompatible structure that can be seeded with the patient's own MSCs to produce an autologous vascular graft.

Keywords

Amnion, Tissue Engineering, Decellularization, Mesenchymal Stem Cells, Corrective Heart Surgery.

For Peer Review ONLY/ Not for Distribution

Mary Ann Liebert, Inc.,140 Huguenot Street, New Rochelle, NY 10801

Impact statement

This study aimed at developing an amnion-based scaffold suitable for vascular tissue engineering applications and in vivo usage. We successfully produced a multi-layered scaffold with improved biomechanical properties and biocompatibility for in vivo vascular implantation. Our approach, not only, offers an allogeneic 'off-the-shelf' solution for clinical use, but it also provides the possibility of personalized medicine by using a patient's own amnion and stem cells for the production of a tissue engineered grafts for reconstructive heart surgery.

For Peer Review ONLY// Not for Distribution

Mary Ann Liebert, Inc.,140 Huguenot Street, New Rochelle, NY 10801

For Peer Review ONLY/Not for Distribution

INTRODUCTION

Congenital heart disease (CHD) is characterized as a heart, aortic, or large blood vessel malformation. Each year, more than one million children worldwide are affected [1], [2]. More than 40 different types of defects have been described, ranging from common, ventricular septal defects (VSD) to the severe tetralogy of Fallot [1], [3]. In the most severe cases, surgery is the only therapeutic option, especially as tissue for transplantations are rare. These surgeries involve using allografts, xenografts, or synthetics to create new conduits and patches in the heart. Allografts and xenografts are the current clinical standard but, like synthetics, they lack longevity, especially when implanted in immature hearts [4]. All these materials do not grow, repair, or remodel with the patient requiring multiple surgeries throughout their lifetime [5].

Tissue engineering offers an alternative source of implants by combining a biofunctional scaffold with allogeneic or autologous stem cells. An ideal scaffold would be nonimmunogenic, nonthrombotic, biocompatible, and have growth and remodeling potential [6]. This scaffold should also have a durable extracellular matrix that can survive in vivo blood pressures. Human amniotic membrane offers a potential scaffold as it is an easily obtainable biologic material that has been used for over a century in skin repair and burn treatment [7], [8]. Later, it was employed for conjunctiva repair [9]. It has been tested in animal models for urethra repair, ocular surface reconstruction, liver repair, and pericardial closure [10]–[13]. In human patients, it has been used for lower eyelid repair, fistula closures, and neovagina construction [14]–[16]. Additionally, it has been shown that amnion has anti-inflammatory and anti-microbial properties [17]–[21].

Bio-functional extracellular matrix is critical in a scaffold for it to be effective in tissue engineering. Studies have demonstrated that the amnion's extracellular matrix is primarily composed of collagen, which is conducive to wound healing, as well as fibronectin, proteoglycans, laminins, and

glycosamnioglycans [17], [22], [23]. Although in most studies the amnion have been used without much modification other than dehydration, several investigations have decellularized it beforehand using a range of approaches including freeze-thawing[24], [25], EDTA[26], and trypsin-EDTA treatment[12], [13]. The latter method retained structural matrix proteins such as collagen type I and IV, fibronectin, and laminin[12], [27]. Many studies have demonstrated successful seeding of decellularized amnion scaffolds with differentiated cells such as human dermal fibroblasts[28], human corneal fibroblasts[25], and smooth muscle cells[24]. Fewer investigations have been carried out to recellularize amnion with stem cells, an approach that could be more promising for tissue engineering purposes.

Long-term amnion preservation is essential for tissue engineering. While matrix preservation was not considered or attempted in many studies [24]–[26], the beneficial effects of preservation were demonstrated by others[28]. Reported preservation work utilized different methods including dehydration[13], [28], refrigeration or freezing[12]. The latter approach resulted in ice crystal formation, contamination, or extracellular matrix protein damage.

In addition to scaffolds, cells represent the second component needed for tissue engineering. Mesenchymal stem cells (MSCs) have been isolated from multiple sources such as bone marrow and adipose tissue [29]. Critically for congenital heart defect repair, MSCs have also been isolated from cord blood and thymus tissue [30]–[32]. MSCs are promising for seeding onto scaffolds as part of a tissue engineered construct for cardiac repair because of their multilineage differentiation potential, ability to regulate the immune response, and because they do not cause teratomas [33]–[35].

Here, we combined a decellularization and freeze-drying approach to produce an amnion based scaffold suitable for tissue engineering constructs destined for reconstructive heart surgery application. Our data showed in vitro and in vivo biocompatibility of the developed amnion-based construct and its suitability for use in pulmonary artery position. Our developed preserved construct offers an ‘off-the-

For Peer Review ONLY / Not for Distribution

shelf' solution for allogeneic clinical use. Furthermore, it represents a key component for personalized medicine, which is possible by using a patient's own amnion and stem cells for the construction of a tissue engineered graft.

For Peer Review ONLY/ Not for Distribution

Mary Ann Liebert, Inc.,140 Huguenot Street, New Rochelle, NY 10801

For Peer Review ONLY/Not for Distribution

MATERIALS AND METHODS

Ethics

Human tissue was collected from patients in compliance with the Human Tissue Act. Perinatal and leftover material (the thymus, cord blood, and placenta) were obtained with parents' consent under NHS ethics license (REC ref. 06/Q2001/197 and 11/SW/0122).

Amnion Preparation

Amnion was collected from 25 human cesarean sections. Amnion (AM) was removed from the fetal side of the placenta by blunt dissection. It was washed once in PBS and then repeatedly with water. It was then stored overnight at 4^{o}C in PBS.

Amnion Decellularization

AM was decellularized in 6-well crown inserts (Scaffdex). Crowns were placed in 0.1% trypsin in 10 mM Tris (Sigma) buffer pH 8.0 and incubated for 3 hours at 37^{o}C under gentle rotation. The solution was changed to 500 U/mL DNase (Sigma) in 10 mM Tris buffer and incubated for an additional 3 hours at 37^{o}C under gentle rotation. Decellularized-AM (d-AM) was then washed in 10 mM Tris buffer every day for 5-9 days at 37^{o}C under gentle rotation.

Tissue Preservation

AM and d-AM were preserved in single or multiple layers by removing from crowns and freezing at -20^{o}C. For freezing, excess liquid was removed, and samples were laid completely flat. Multi-layer samples were stacked, cross-sectionally, on top of each other and all air bubbles were removed. They were then freeze-dried (fd; Edwards) and stored at room temperature. These single (d-AM-fd-single)

and multi-layered (d-AM-fd-multi) constructs were rehydrated in respective cell culture mediums prior *in vitro* testing.

Thymus Derived Mesenchymal Stem Cells

Thymus tissue was collected from patients undergoing congenital heart surgery and placed in sterile PBS from the surgical theatre. The thymus was washed in PBS (Life Technologies), minced into small pieces, and underwent a 2 hours collagenase I (Sigma-Aldrich, 0.3 mg/mL) enzymatic digestion. The digested tissue was forced through a strainer and was washed with fresh medium. The resulting cell suspension was centrifuged for 5 minutes at 420 x g at 22^{o}C. The supernatant was discarded and cells were resuspended in Dulbecco's Modified Eagle Medium, low glucose (DMEM, Life Technologies) with 10% HyClone Fetal Bovine Serum (FBS, Thermo Scientific), 1% penicillin streptomycin (p/s, Life Technologies) on uncoated plastic, at approximately 1x10^{6} cells/cm^{2} density in a 37^{o}C humidified atmosphere with 5% CO_2. After 72-96 hours, non-adherent cells were removed with two PBS washes. Adherent cells were cultured until confluence was reached, with feeding every 48-72 hours. At this point, cells were detached using Trypsin-EDTA (0.05%, Life Technologies) and then plated at approximately 1x10^{4} cells/cm^{2} in new flasks for next passage (P1).

Umbilical Cord Blood Mesenchymal Stem Cells

Human umbilical cord blood was collected in 1% herparin (LeoPharma) from consenting patients undergoing caesarean section. Blood was diluted 1:2 with P/S PBS and layered onto Ficoll (GE Healthcare). Tubes were centrifuged at 400 x g at room temperate for 30 minutes with no brake. Mononuclear cells were removed with a 10 mL syringe and washed three times with P/S PBS. Finally, they were spun at 420 x g for 5 minutes and the supernatant was discarded. Cells were plated at approximately 1x10^{6} cells/cm^{2} on uncoated plastic and cultured in 95% air, 5% CO_2, and 37^{o}C. Non-

Mary Ann Liebert, Inc.,140 Huguenot Street, New Rochelle, NY 10801

For Peer Review ONLY / Not for Distribution

adherent cells were removed by washing with PBS after 72-96 hours. Adherent cells were cultured with DMEM, 10% FBS, 1% P/S with media changes every 48-72 hours.

Human Umbilical Vein Endothelial Cells

Human umbilical cord vein (hUVEC) cells were purchased from Lonza. They were cultured on uncoated plastic in 95% air, 5% CO_2, and 37^{o}C in Endothelial Cell Growth Medium (PromoCell), with media changes every 48-72 hours.

Cardiac Myocytes

Cardiac Myocytes were purchases from PromoCell. They were cultured on uncoated plastic in 95% air, 5% CO_2, and 37^{o}C in Cardiac Myocyte Growth Medium (PromoCell) according to manufacturer's instructions.

Arterial Smooth Muscle Cells

Smooth muscle cells were collected from the artery of the umbilical cord. Cord was cut open, arteries were removed and cleaned in PBS, and chopped into pieces. Artery pieces were then cultured in DMEM, 10% FBS, 1% P/S in 95% air, 5% CO_2, and 37^{o}C. Smooth muscle cells were outgrown from these arterial pieces in 10 cm petri dishes.

AM cell seeding

AM, d-AM, d-AM-fd-single and d-AM-fd-multi were sterilized under 295 nm UV for 30 minutes on each side. They were then seeded with each cell type at 250,000 cells/cm^2 in respective culture mediums. Cell-seeded AM was cultured for 1 week at 37^{o}C in a humidified atmosphere with 5% CO_2 with medium changes every 2-3 days. Apart from hUVEC and cardiac myocytes (commercially sourced) a different cell line, prepared from a different sample, was used for each experimental point.

For Peer Review ONLY// Not for Distribution

For Peer Review ONLY/Not for Distribution

Cell Viability

To test cell viability on scaffolds, the Live/Dead Viability/Cytotoxicity Kit, for mammalian cells (ThermoFisher) was used according to manufacturer's instructions with Hoechst (ThermoFisher, 1ng/mL) in PBS. Samples were imaged on a Zeiss Axio Observer.Z1 with Zen Blue software (Zeiss). Cell counts were performed using ImageJ.

Immunohistochemistry

For tissue analysis, samples were embedded in paraffin. First, they were fixed in 4% PFA, washed in PBS, moved in to cassettes (Histosette I, Symports), processed in a Thermo Excelsior AS, and embedded in a Thermo HistoStar machine. Sections were cut on a microtome (Thermo) at 5 µm, floated onto Menzel-Glaser SuperFrost Plus slides (Thermo), and dried overnight. Hematoxylin and eosin (H&E) and van Gieson's (EVG) stains were performed using a Shandon Varistain 24-4 (Thermo). Slides were removed from machine and mounted with DPX (distyrene, a plasticizer, in toluene-xylene; Sigma). Slides were imaged on a Zeiss Axio Observer.Z1 with Zen Blue software (Zeiss).

For immunofluorescence analysis, samples were deparaffinized in clerene and rehydrated through an alcohol gradient. Antigen retrieval was performed with 10 mM citrate buffer pH 6.0 heated to boil. 10% goat serum (Sigma-Aldrich) in PBS was used to block the samples for 30 minutes at room temperature. Samples were incubated with the primary antibodies overnight at 4°C. Antibody solutions were prepared as follow: 1:100 Isolectin-B4-biotin (Life Technologies), 1:200 mouse to alpha-smooth muscle actin (Abcam), 1:100 mouse to smooth muscle-myosin heavy chain (Dako) and 1:100 rabbit to calponin (Dako). Secondary antibodies were then incubated on the sections for 1 hour at room temperature in the dark. The secondary antibodies used were as follow: 1:200 streptavidin-Alexa Flour 488 (Life Technologies), 1:300 goat-anti-mouse-Cy3 (Jackson Immuno Research Labs), 1:400 goat-anti-mouse-

Alexa Flour 488 (Abcam) and 1:400 goat-anti-rabbit-Alexa Flour 546 (Abcam). Dapi was used to counterstain the nuclei and the slides were mounted using Hardset mounting medium (Vectashild).

Scanning Electron Microscopy

Tissue samples were prepared by fixing in 2.5% glutaraldehyde in sodium cacodylate buffer (Electron Microscopy Sciences) for 45 minutes. Following fixation, samples were washed 3 times in 0.1 M sodium cacodylate buffer (from Cacodylate acid, Sigma). Osmium (Electron Microscopy Sciences) solution was prepared with 1% osmium in 0.1 M sodium cacodylate buffer and put on samples for 20 minutes. Samples were washed and dehydrated as follows: three changes of 0.1 M sodium cacodylate; one each of water; 25%, 50%, 70%, 80%, 90%, 96% ethanol; and 3 three changes of 100% ethanol with each step 10 minutes at room temperature. Samples were dried completely in the critical point dryer (Leica EM CPD300) and mounted on stubs (Agar Scientific) with 12 mm carbon tabs (Agar Scientific). They were then coated at 100 mA for 30 seconds using an EMITECH K575X sputter coater. Surface details were imaged using a Quanta 200 FEI field emission scanning electron microscope.

Mechanical Testing

Samples were analyzed for mechanical properties with pneumatic grips and a 100 N load cell on an Instron 3343B machine. Crosshead speed was 10 mm/min. Samples were measured for tensile stress at break and Young's Modulus using Bluehill software (Instron).

In vivo implantation of the multilayered decellularized-freeze-dried amnion

Two three ~~to four~~ weeks-old female Landrace pigs of 10-15 kg were employed in this study. No mortality was recorded. Animals were treated in accordance with the "Guide for the Care and Use of Laboratory Animals" published by the National Institutes of Health in 1996 and conforming to the "Animals (Scientific Procedures) Act" published in 1986. Surgical procedures were performed under general

For Peer Review ONLY/ Not for Distribution

anaesthesia and neuromuscular blockade (Pancuronium Bromide, 2 mg/ml). Anaesthesia was induced by intramuscular injection of 15 mg/kg Ketamine, 0.4 mg/kg Midazolam and 5 mg/kg Dexmedetomidine and then maintained with inhalation of 1-2% Isoflurane. A left postero-lateral thoracotomy was performed and ~~a~~ patches of different multilayered freeze-dried amnions were ~~was~~ inserted in the Left Pulmonary Arteries. Both animals were successfully recovered from the surgical procedures and ~~with~~ intensevely monitored ~~ing~~ for 24 hours. Analgesic and antibiotics were administered according to the needs. A combination of 10 mg/kg Paracetamol, 0.2 mg/kg Morphine, 20 mg/kg Cefuroxime and 0.4 mg/kg Meloxicam were regularly administered intravenously during this period. The animals were monitored with a two-dimensional Doppler Echocardiography (VividQ, GE Healthcare) prior the surgery, immediately after the surgery and after 2.5 months in order to assess the LPA patency and blood flow at the level of the patch. After 2.5 months of follow up, pigs were euthanized with an intravenous injection of 150 mg/kg Euthatal. The ~~and~~ pulmonary arteries were dissected from the heart and then fixed in 4% PFA or fresh-frozen in liquid nitrogen.

Statistical Tests

Statistical testing was carried out with t-test or one-way ANOVA with Tukey post-hoc testing as appropriate, using R. A value of $p < 0.05$ was considered statistically significant.

For Peer Review ONLY // Not for Distribution

For Peer Review ONLY / Not for Distribution

RESULTS

Amnion dissection and composition

Human placenta was collected, dissected, and cleaned to isolate the control amniotic membrane (AM) (**Figure 1 a**). The native epithelial cell layer had a cobblestone-like morphology, which was observed on the surface of the amnion using scanning electron microscopy (**Figure 1 b**). Histological characterization was performed using H&E and EVG staining. H&E showed a single layer of epithelial cells on the surface of the membrane (**Figure 1 c**) while EVG indicated a collagen matrix (**Figure 1 d**).

The surface of the control non-processed amnion does not allow survival and growth of seeded MSCs

Thymus derived mesenchymal stem cells were isolated and seeded on the surface of the AM. Cell viability staining demonstrated the lack of viable cells (green Calcein fluorescence). Numerous nuclei were observed on the surface; however, all were positive for Ethidium III (red) indicating cell death of the amnion's epithelial cells as well as seeded cells. There was no observed positive calcein (green) staining for viable seeded cells, showing that MSCs did not survive on the matrix, due either the lack of adherence because of the presence of residual epithelial cells or perhaps the presence of factors released by the dying native AM cells that triggered MSC cell death (**Figure 1 e**). The scanning electron micrographs still showed a similar cobblestone-like morphology, but the epithelial cells appeared damaged; smooth, elongated MSCs were not observed (**Figure 1 f**). H&E cross-sections of AM-seeded grafts illustrated the epithelial cells on the surface of the AM but no additional cells (**Figure 1 g**). Collagens were intact as shown by EVG ~~however, no new collagens produced by seeded cells were visible~~ (**Figure 1 h**). In summary, the seeded MSCs did not adhere or survive on the surface of the AM. The latter only showed dead epithelial cells on the surface.

For Peer Review Only / Not for Distribution

Trypsin decellularization completely removed epithelial cells and allowed for MSC adherence and survival ~~and growth~~

Trypsin decellularized amnion (d-AM) was stained with viability stain and H&E to verify removal of cellular components (**Figure 2 a ~~, b~~**). No nuclear stain was detected. Furthermore, the epithelial cells were no longer visible on the surface of the matrix confirming successful decellularization with no visible cells or cell fragments (**Figure 2 a)**. EVG demonstrated no disruption to the matrix following treatment; the collagens were preserved (**Figure 2 a ~~c~~**). Extracellular matrix fibers made up the surface of the matrix, as visualized by scanning electron micrographs (**Figure 2 a ~~d~~**). MSCs seeded on the surface of the decellularized matrix were viable (**Figure 2 a ~~e~~**). The elongated structure of the cells indicated the survival of the MSCs. Nuclei were observed on the surface of cross-sections H&E ~~images~~, though in small numbers (**Figure 2 a ~~f, arrows~~**). EVG showed an intact collagen matrix though with a small amount of loose collagen that could potentially be made by seeded cells ~~deposition~~ (**Figure 2 a ~~g~~**). Surface micrographs illustrate elongated MSCs on the surface of the d-AM, with a few extracellular matrix fibers still visible between the cells (**Figure 2 a ~~h~~**).

Preservation of the Amnion as a single and multi-layered structure resulted in better growth of seeded cells

For long-term preservation of the matrix, the d-AM was freeze-dried as a single or a multi-layer. Single layer decellularized freeze-dried amnion (d-AM-fd-single) and multilayer decellularized freeze-dried amnion (d-AM-fd-multi) produced a paper-like structure (**Figure 2 b ~~i & q~~**, respectively). H&E staining ~~again~~ illustrated no residual cellular material in d-AM-fd-single (**Figure 2 b ~~j~~**) while EVG demonstrated that the collagens became more compact (**Figure 2 b ~~k~~**). The compact collagen fibers of the extracellular matrix are visible in the scanning electron micrograph (**Figure 2 b ~~l~~**).

Cell survival was then tested on the d-AM-fd-single seeded with MSCs. After seven days in culture, viability staining showed elongated viable MSCs (**Figure 2 c ~~m~~**). This layer of cells is also seen in the cross-section of the H&E (**Figure 2 c ~~n~~**). Loose ~~and the production of new~~ collagens are ~~is~~ shown in the EVG (**Figure 2 c ~~o~~**). The scanning electron micrographs show confluent MSCs layer on the surface of the preserved matrix (**Figure 2 c ~~p~~**).

For improving the ease of handling and strength, the material was then layered (d-AM-fd-multi) (**Figure 2 b ~~q~~**). The d-AM-fd-multi had no residual nuclear material, as shown by H&E (**Figure 2 b ~~r~~**). EVG showed the collagens were undamaged but again became far more compact (**Figure 2 b ~~s~~**). Surface morphology indicated extracellular matrix fibers much the same as after decellularization (**Figure 2 b ~~t~~**). These results indicate that the matrix could be preserved and handled by layering and freeze-drying.

d-AM-fd-multi was then tested for seeded cell survival. Cell viability indicated extensive cell population after one week in culture (**Figure 2 c ~~u~~**). This was further confirmed by H&E staining which showed 2-3 ~~multiple~~ cells layer on the surface of the d-AM-fd-multi (**Figure 2 c ~~v~~**). The EVG demonstrated loose ~~moderate new~~ collagen ~~production with pink fibers~~ above the compact layers of amnion suggesting that this collagen could be newly made by the seeded cells (**Figure 2 c ~~w~~**). The cells on the surface in the scanning electron micrographs were compact and extracellular matrix fibers were no longer visible (**Figure 2 c ~~x~~**). The cell population growth ~~was more robust~~ on the freeze-dried matrixes (d-AM-fd-single, d-AM-fd-multi) was as good (if not slightly better in case of d-AM-fd-multi) as growth ~~than~~ on wet decellularized amnion (d-AM) that was not freeze-dried.

Quantification of Cell Survival on the Surface of the Decellularized Amnion

Control amnion was freeze-dried (AM-fd) and rehydrated to be directly comparable to decellularized d-AM-fd-single-seeded and d-AM-fd-multi-seeded. The cell survival and viability of the MSCs on the surface of the AM-fd was compared to d-AM-fd-single and d-AM-fd-multi (**Figure 3**). Cell viability images

For Peer Review ONLY/ Not for Distribution

were counted for the number of green, viable cells. Representative AM-fd-seeded (**Figure 3 a**), d-AM-fd-single seeded (**Figure 3 b**), and d-AM-fd-multi-seeded (**Figure 3 c**) images show fewer viable cells on the dry-AM-seeded as compared to the d-AM-fd-single-seeded and d-AM-fd-multi-seeded. The data demonstrated significantly higher cell viability on the surface of the d-AM-fd-single-seeded (430.7 ± 32.3 cells/mm^2, n=3, technical triplicate) and d-AM-fd-multi-seeded (543.4 ± 70.5 cells/mm^2, n=7, technical triplicate) than on the AM-fd-seeded (168.4 ± 35.8 cells/mm^2, n=6, technical quadruplet; p=0.023 and p<0.001 respectively, **Figure 3 d**). There was no significant difference between the d-AM-fd-single and d-AM-fd-multi-seeded (p=0.45, one-way ANOVA, Tukey post-hoc testing).

Mechanical Strength of the Amnion

The ~~uniaxial~~ ultimate tensile strength ~~stress~~ (UTS) and Young's Modulus were calculated to determine the strength and elasticity of the different engineered amnion constructs (**Figure 4**). Amnion was measured and pulled to break point to determine the UTS ~~ultimate tensile strength~~ (**Figure 4 a**). The native, AM, was compared to the d-AM, the d-AM-fd-single, the d-AM-fd-multi, and the d-AM-fd-single and d-AM-fd-multi which had been seeded with MSCs and was in culture for 7 days (d-AM-fd-single-seeded and d-AM-fd-multi-seeded). AM (1.94 ± 0.20 MPa), d-AM (1.98 ± 0.27 MPa), d-AM-fd-single (2.47 ± 0.24 MPa) and d-AM-fd-single-seeded (1.17 ± 0.19 MPa) had the lowest UTS with no significant difference in values. The d-AM-fd-multi (7.33 ± 1.15 MPa) and the d-AM-fd-multi-seeded (6.49 ± 1.22 MPa) had significantly higher UTS than AM ($p < 0.0001$; $p = 0.004$), d-AM ($p < 0.0001$; $p = 0.011$), d-AM-fd-single ($p < 0.0001$; $p = 0.021$), and d-AM-fd-single-seeded ($p < 0.0001$; $p = 0.0126$) respectively. No significant difference in UTS was observed when comparing the unseeded d-AM-fd-multi and d-AM-fd-multi-seeded ($p = 0.96$). Young's Modulus for the different materials were also calculated (**Figure 4 b**). The d-AM-fd-multi had the highest Young's Modulus (116.4 ± 22.2 MPa) and was significantly different to Young's Modulus of AM (28.0 ± 2.8; $p < 0.0001$), d-AM (36.1 ± 5.6; $p = 0.00044$), d-AM-fd-single (46.9

For Peer Review ONLY / Not for Distribution

± 5.2; p = 0.00077), and d-AM-fd-single-seeded (21.3 ± 4.1; p = 0.0033). There was no significant difference between the d-AM-fd-multi and the d-AM-fd-multi-seeded (77.1 ± 14.3) and no other significant differences were noted in the other comparisons. All the tested materials had UTS and Young's modulus values higher than those of native left pulmonary artery (UTS= 0.46MPa, Young's modulus=1.40MPa).

d-AM-fd-multi supports cell survival ~~growth~~ of other cell types

MSCs isolated from human umbilical cord blood (hUCB-MSCs) represent another population of cells for tissue engineering applied to congenital heart defect corrective surgery. These cells were expanded and seeded on the surface of the d-AM-fd-multi matrix. The hUCB-MSCs survived on the matrix ~~and proliferated~~ as demonstrated by viability ~~staining (**Figure 5 a**)~~ and H&E stainings (**Figure 5 a**). The seeded cells ~~began to produce their own extracellular matrix (**Figure 5 c**) and~~ completely covered the surface of the material as shown by SEM ~~scanning electron micrographs~~ (**Figure 5a ~~d~~**). Human umbilical vein endothelial cells (hUVECs)~~, characterized with von Willebrand Factor (VWF) and CD31 staining (**Supplement 1**)~~ were also able to survive on the matrix (**Figure 5a ~~e~~**) and created a sparse cell layer on the surface of the material as shown by H&E and SEM (**Figure 5a ~~f, h~~**) ~~and collagen layer (**Figure 5 g**)~~. Smooth muscle cells offer a potential for vascular tissue engineering. Smooth muscle cells isolated from umbilical artery were ~~characterized with smooth muscle actin (SMA), calponin, and myosin heavy chain (**Supplement 1**) then~~ seeded on the surface of the d-AM-fd-multi. These smooth muscle cells survived ~~(**Figure 5i**)~~ and covered ~~populated~~ the matrix as shown by live cells staining , H&E and SEM (**Figure 5b ~~j, l~~**) ~~and created a collagen layer (**Figure 5 k**)~~. Cardiac myocytes are another important cell type for congenital heart defect repair. ~~and were characterized with connexin 43 and desmin staining (**Supplement 1**)~~. Seeded cardiac myocytes survived and covered ~~on~~ the surface of the matrix as shown

For Peer Review ONLY Not for Distribution

by live cells staining , H&E and SEM (**Figure 5b ~~m~~**). ~~and created a cell layer (**Figure 5 n, p**). These cells also began to produce collagens (**Figure 5 o**).~~

Proof-of-concept: d-AM-fd-multi shows in vivo integration and regeneration of vascular tissue

In order to assess the in vivo biocompatibility of the developed multilayered freeze-dried amnion-scaffold, a piglet model of left pulmonary artery (LPA) grafting was used (**Figure 6 a**). A small cut was made in the left pulmonary arteries of two piglets and two different ~~the~~ d-AM-fd-multi constructs were ~~was~~ inserted. Immediately after the surgery (**Figure 6 b**) and at 2.5 months post-operatively the LPA was patent with no stenosis or rupture (**Figure 6 d**). Macroscopic inspection of the graft after explantation demonstrated smooth luminal surface with no sign of thrombosis and tissue degradation (**Figure 6 c**). The blood velocity through the LPA, assessed by Doppler, showed maximum values less than 2.5m/s indicating normal blood flow. These results were similar to the blood flow through the LPA immediately prior to surgery (**Figure 6 d**). Histological assessment of the graft demonstrated extensive nucleation throughout its structure (**Figure 6 e**). Graft thickness resembled the neighboring native LPA, although not quite as thick (**Figure 6 e**). Histological assessment of inflammation in the graft showed no inflammatory cells within the newly formed tissue and away from sutures (**Figure 6 f**). However inflammatory cells, mainly lymphocytes and granulocytes, were present near the sutures (**Figure 6 f**). The presence of Inflammatory cells near sutures is common following cardiovascular surgery. The inner side of the graft exhibited a newly-formed organized endothelial cells layer as shown by SEM and cross sections isolectin ~~immuno~~ staining ~~and scanning electron microscopy~~ (**Figure 6 g, h ~~f~~,**). The immuohistochemical analysis of graft cross-sections demonstrated an organized multilayer of smooth muscle cells comparable to the native left pulmonary artery as illustrated by alpha-smooth muscle actin, smooth muscle myosin heavy chain, and calponin staining indicating a vessel-like phenotype (**Figure 6 h ~~g~~**). Finally, new vessels (vasa vasorum) were observed in the adventitia of the graft indicating neo-

For Peer Review ONLY/ Not for Distribution

vascularization that is crucial for oxygen and nutrients supply to the graft **(Figure 6 i ~~e~~)**. These results provide evidence of the suitability of our amnion-derived construct for in vivo use and particularly for vascular repair application.

For Peer Review ONLY/ Not for Distribution

DISCUSSION

Amniotic membrane has been used for over a century now. Its use was warranted by its easy and wide availability as well as its anti-microbial and anti-inflammatory properties. Here we developed a method that produced an amnion-derived construct that is biocompatible and strong enough for cardiovascular application. Our adopted strategy to decellularize then freeze-dry the amniotic membrane improved the viability of the seeded cells as compared to non-freeze-dried non-decellularized material and offered a method of preservation and storage that is critical for an "off-the-shelf" clinical product. Additionally, layering the decellularized amnion, during the freeze-drying process, created a 4-ply construct with significantly improved tensile strength and elasticity that made it possible to use in preclinical reconstructive heart surgery.

Using our amnion-derived graft as a patch inserted in the left pulmonary artery of a piglet model demonstrated clear in vivo suitability. The grafted LPA was patent and exhibited normal blood flow up to 2.5 months post-operatively. Additionally, the explanted graft displayed a newly formed endothelium in the intima, a ~~and~~ smooth muscle cell-rich medial layer and an adventitia containing new vasa vasorum. Using preserved human amnion with thymus-derived MSCs, a completely autologous graft could be constructed for use in corrective heart surgery for congenital heart defect patients.

The observed limited cell growth on the surface of native amnion led us, like others [28], to use decellularization as a way to improve cell viability and growth on this material. Our data demonstrated the advantage of decellularization for mesenchymal stem cells' growth on decellularized amnion. Similar results were obtained when seeding differentiated fibroblasts on decellularized and non-decellularized amnion [28]. Another advantage of decellularization of the amnion is to reduce immune response in the recipient if used in an allogeneic manner.

Mary Ann Liebert, Inc.,140 Huguenot Street, New Rochelle, NY 10801

For Peer Review ONLY / Not for Distribution

A variety of techniques have been used to decellularize the amnion [15], [24], [26], [28]. We optimized a trypsin-EDTA, nuclease decellularization protocol that eliminated cell and nuclear materials from the amnion. While, other groups have used their amnion material for body surface repair like foot ulceration repair[36], [37], lower eyelid repair[16], and fistula reconstruction[15], we have focused on an internal cardiovascular application for our developed amnion based bioscaffold.

For cardiovascular reconstructive surgery, porcine materials have commonly been used for cardiovascular repair because of their wide availability and good mechanical properties. Decellularization is frequently used to remove porcine cells' remains that could trigger an immune response in the human recipient[38]–[40]. When decellularization is incomplete, it can result in rejection, in the recipient patient, due to the galactose-α1-3galactose (α-gal) epitope present on non-human mammalian cells[39], [41]. The human amnion offers an alternative ~~better~~ solution for some applications with the advantage that ~~as~~ it ~~obviously~~ doesn't contain the α-gal epitope that could be responsible for triggering the immune response. Additionally, using a patient's own autologous tissue could represent a further improved solution as it prevents other potential allogeneic immune response. For these reasons decellularized amnion represent a good ~~safer~~ alternative to non-human tissue-derived scaffolds.

This is the first study, to our knowledge, where the decellularized amniotic membrane has been prepared by preserving layered tissue, tested for cell seeding to form a tissue engineered construct, and finally tested for biocompatibility, feasibility and safety in an in vivo vascular repair model. The pig model is an ideal organism for in vivo testing of cardiovascular grafts because of its rapid growth potential and cardiovascular anatomy similar to human. Preservation of the matrix allows for an 'off-the-shelf' solution that can be easily transported and used. It also results in improved cell survival compared to control dehydrated matrix. Our developed protocol is scalable in a setting where amnion

For Peer Review ONLY/Not for Distribution

harvest is carried out systematically with a streamlined ethical approval. However, scalability wouldn't be an issue for using the material in an autologous manner where a patient's own amnion and stem cells will be used for producing a tissue engineered grafts.

EpiFix is a commercially available dehydrated amnion, equivalent to our control dehydrated matrix. The manufacturer suggests that keeping the amniotic membrane intact (non-decellularized) would help preserve the cytokines useful for regenerating damaged tissue[42]. In our in vitro system, cell adherence and viability were very poor when MSCs were seeded on non-decellularized amnion. They improved dramatically when MSCs were seeded on decellularized material. These results question the advantage of not decellularizing the amniotic membrane. Furthermore, our in vivo experiment using decellularized bioscaffold showed infiltration of endothelial cells in the intima and smooth muscle cells in the media of the graft. Cell infiltration is a crucial process for tissue regeneration and decellularizing the amnion seems to be compatible with this process. In support of our results, it has been reported that when non-decellularized amnion was applied to ischemic rat hearts, no cell infiltrated was observed after 90 days in vivo[43]. Other in vivo work using non-decellularized amnion has shown inflammatory infiltrate[10], [20]. Decellularization may have removed cytokines from the amnion but the remaining extracellular matrix seems to sufficiently support cell infiltration and regeneration in vivo. Additionally, seeding MSCs on the decellularized amnion should further improve the regenerative capacity of the tissue engineered graft.

Consistent with previous findings, no significant difference in tensile strength was found following decellularization[44]. We showed, as it has previously been demonstrated, that the collagens and extracellular matrix proteins in the extracellular matrix are not damaged by the decellularization process[27]. The strength of the amnion was not compromised when decellularized or after drying for preservation. Furthermore, its tensile strength improved significantly when it was dried and layered.

Mary Ann Liebert, Inc.,140 Huguenot Street, New Rochelle, NY 10801

For Peer Review ONLY/Not for Distribution

This strength was important for in vivo implantation in a vessel position. After 2.5 months, the preserved amnion-derived graft was still intact and able to withstand the in vivo blood pressure. Further, it integrated well within the surrounding left pulmonary artery tissue and displayed a typical vessel-like structure composed of intima, media and adventitia. Other natural materials, such as decellularized carotid arteries and small intestine submucosa extracellular matrix, have shown similar results. When seeded and implanted in vivo, the grafts displayed an inner luminal layer, a medial smooth muscle layer, and some adventitia [32], [45]. Similar results were obtained by using synthetic scaffolds seeded with bone marrow mononuclear cells[46].

Babies born with heart defects usually need surgery within the first six months of life and using reconstructive materials with growth and remodeling capacity, would reduce the number of surgeries the child has to endure. The growth potential of our developed construct remains to be tested in further investigations. However, our proof of concept in vivo study demonstrates a remodeling potential for this material. While the non-anti-microbial and anti-inflammatory properties[17], [18] of our amnion based-construct warrant potential allogeneic use, these properties could be further improved by potentially using the patient's own amnion collected at birth (autologous use).

In conclusion, we successfully produced a multi-layered scaffold with biomechanical properties and biocompatibility suitable for in vivo vascular implantation. Our approach, not only, offers an allogeneic 'off-the-shelf' solution for clinical use, but it also provides the possibility of personalized medicine by using a patient's own amnion and stem cells for the production of a tissue engineered grafts for reconstructive heart surgery.

Acknowledgments

For Peer Review ONLY/Not for Distribution

This study was supported by the Sir Jules Thorn Charitable Trust, the Enid Linder Foundation, the British Heart Foundation and the NIHR Bristol Biomedical Research Centre.

Declaration of Conflict of Interest

The authors have no conflicts of interest to disclose.

Author contributions

MTG and MC conceived and designed the research. MMS performed the in vitro experiments. MC, MTG, AA and DI carried out the animal work. MMS, MTG and AA analyzed data. MMS and MTG interpreted results of experiments. MMS prepared figures. MMS and MTG drafted and edited the article. MTG, MMS, MC, AA and DI revised the article. All authors read and approved the final version of manuscript.

For Peer Review ONLY // Not for Distribution

Mary Ann Liebert, Inc.,140 Huguenot Street, New Rochelle, NY 10801

REFERENCES

[1] The Children's Heart Foundation, "Fact Sheet," 2012. [Online]. Available: http://childrensheartfoundation.org.

[2] P. I. Aaronson and J. P. T. Ward, *The Cardiovascular System at a Glance*, 3rd ed. Oxford: Blackwell Publishing, 2007.

[3] J. I. E. Hoffman and S. Kaplan, "The incidence of congenital heart disease.," *J. Am. Coll. Cardiol.*, vol. 39, no. 12, pp. 1890–900, Jun. 2002.

[4] Z. Mosala Nezhad, A. Poncelet, L. de Kerchove, P. Gianello, C. Fervaille, and G. El Khoury, "Small intestinal submucosa extracellular matrix (CorMatrix®) in cardiovascular surgery: a systematic review.," *Interact. Cardiovasc. Thorac. Surg.*, vol. 22, no. February, pp. 839–850, 2016.

[5] A. Quarti, S. Nardone, M. Colaneri, G. Santoro, and M. Pozzi, "Preliminary experience in the use of an extracellular matrix to repair congenital heart diseases.," *Interact. Cardiovasc. Thorac. Surg.*, vol. 13, no. 6, pp. 569–72, Dec. 2011.

[6] E. Avolio, M. Caputo, and P. Madeddu, "Stem cell therapy and tissue engineering for correction of congenital heart disease," *Front. Cell Dev. Biol.*, vol. 3, no. June, pp. 1–17, Jun. 2015.

[7] N. Sabella, "Use of the fetal membranes in skin grafting," *Med. Rec.*, vol. 83, pp. 478–480, 1913.

[8] M. Stern, "The Grafting of Preserved Amniotic Membrane to Burned and Ulcerated Surfaces, Substituting Skin Grafts," *J. Am. Med. Assoc.*, vol. 60, pp. 973–974, 1913.

[9] A. de Rotth, "Plastic Repair of Conjunctival Defects with Fetal Membranes," *Arch. Opthalmol.*, vol. 23, pp. 522–525, 1940.

Mary Ann Liebert, Inc.,140 Huguenot Street, New Rochelle, NY 10801

For Peer Review ONLY Not for Distribution

[10] S. Muralidharan, J. Gu, G. W. Laub, R. Cichon, C. Daloisio, and L. B. McGrath, "A new biological membrane for pericardial closure," *J. Biomed. Mater. Res.*, vol. 25, pp. 1201–1209, 1991.

[11] T. Nakamura, M. Yoshitani, H. Rigby, N. J. Fullwood, W. Ito, T. Inatomi, C. Sotozono, T. Nakamura, Y. Shimizu, and S. Kinoshita, "Sterilized, Freeze-Dried Amniotic Membrane: A Useful Substrate for Ocular Surface Reconstruction," *Investig. Ophthalmol. Vis. Sci.*, vol. 45, no. 1, pp. 93–99, 2004.

[12] J. Yuan, W. Li, J. Huang, X. Guo, X. Li, X. Lu, X. Huang, and H. Zhang, "Transplantation of human adipose stem cell-derived hepatocyte-like cells with restricted localization to liver using acellular amniotic membrane," *Stem Cell Res. Ther.*, vol. 6, no. 1, p. 217, 2015.

[13] C. Chen, S. Zheng, X. Zhang, P. Dai, Y. Gao, L. Nan, and Y. Zhang, "Transplantation of Amniotic Scaffold-Seeded Mesenchymal Stem Cells and/or Endothelial Progenitor Cells From Bone Marrow to Efficiently Repair 3-cm Circumferential Urethral Defect in Model Dogs," *Tissue Eng. Part A*, vol. 24, p. ten.tea.2016.0518, 2017.

[14] S. K. Kathpalia, "Creating neovagina using amnion," *Med. J. Armed Forces India*, vol. 72, pp. S120–S122, 2016.

[15] Z. Kakabadze, K. Mardaleishvili, G. Loladze, I. Javakhishvili, K. Chakhunasvili, L. Karalashvili, N. Sukhitashvili, G. Chutkerashvili, A. Kakabadze, and D. Chakhunasvili, "Clinical application of decellularized and lyophilized human amnion/chorion membrane grafts for closing post-laryngectomy pharyngocutaneous fistulas," *J. Surg. Oncol.*, vol. 113, no. 5, pp. 538–543, 2016.

[16] O. J. Wisco, "Case series: The use of a dehydrated human amnion/chorion membrane allograft to enhance healing in the repair of lower eyelid defects after Mohs micrographic surgery," *JAAD Case Reports*, vol. 2, no. 4, pp. 294–297, 2016.

[17] H. S. Dua and A. Azuara-blanco, "Amniotic membrane transplantation," *Br. J. Opthalmology*, vol.

Mary Ann Liebert, Inc.,140 Huguenot Street, New Rochelle, NY 10801

For Peer Review ONLY // Not for Distribution

83, pp. 748–752, 1999.

[18] Y. Hao, D. Hui-Kang, D. G. Hwang, W.-S. Kim, and F. Zhang, “Identification of Antiangiogenic and Antiinflammatory Proteins in Human Amniotic Membrane,” *Cornea*, vol. 19, no. 3, pp. 348–352, 2000.

[19] N. Kjaergaard, M. Hein, L. Hyttel, R. B. Helmig, H. C. Schønheyder, N. Uldbjerg, and H. Madsen, “Antibacterial properties of human amnion and chorion in vitro,” *Eur. J. Obstet. Gynecol. Reprod. Biol.*, vol. 94, no. 2, pp. 224–229, Feb. 2001.

[20] T. Maral, H. Borman, H. Arslan, B. Demirhan, G. Akinbingol, and M. Haberal, “Effectiveness of human amnion preserved long-term in glycerol as a temporary biological dressing,” *Burns*, vol. 25, pp. 625–635, 1999.

[21] Y. P. Talmi, L. M. U. Sigler, E. Inge, Y. Finkelstein, and Y. Zohar, “Antibacterial Properties of Human Amniotic Membranes,” *Placenta*, vol. 12, pp. 285–288, 1991.

[22] D. E. Fetterolf and R. J. Snyder, “Scientific and Clinical Support for the Use of Dehydrated Amniotic Membrane in Wound Management,” *Wounds*, vol. 24, no. 10, pp. 299–307, 2012.

[23] J. Lei, L. B. Priddy, J. J. Lim, M. Massee, and T. J. Koob, “Identification of Extracellular Matrix Components and Biological Factors in Micronized Dehydrated Human Amnion/Chorion Membrane,” *Adv. Wound Care*, vol. 0, no. 0, p. wound.2016.0699, 2016.

[24] S. Amensag and P. S. Mcfetridge, “Tuning scaffold mechanics by laminating native extracellular matrix membranes and effects on early cellular remodeling,” *J Biomed Mater Res A*, vol. 102, no. 5, pp. 1325–1333, 2014.

[25] S. C. Tseng, D. Q. Li, and X. Ma, “Suppression of transforming growth factor-beta isoforms, TGF-

For Peer Review ONLY/Not for Distribution

beta receptor type II, and myofibroblast differentiation in cultured human corneal and limbal fibroblasts by amniotic membrane matrix.," *J. Cell. Physiol.*, vol. 179, no. 3, pp. 325–35, 1999.

[26] F. Chehelcheraghi, H. Eimani, S. Homayoonsadraie, G. Torkaman, H. A. Majd, and H. Shemshadi, "Effects of Acellular Amniotic Membrane Matrix and Bone Marrow-Derived Mesenchymal Stem Cells in Improving Random Skin Flap Survival in Rats," *Iran. Red Crescent Med. J.*, vol. 18, no. 6, pp. 1–11, 2016.

[27] R. A. Salah, I. K. Mohamed, and N. El-Badri, "Development of decellularized amniotic membrane as a bioscaffold for bone marrow-derived mesenchymal stem cells: ultrastructural study," *J. Mol. Histol.*, vol. 0, no. 0, p. 0, 2018.

[28] X. Guo, A. Kaplunovsky, R. Zaka, C. Wang, H. Rana, J. Turner, Q. Ye, I. Djuretic, J. Gleason, V. Jankovic, J. Smiell, M. Bhatia, W. Hofgartner, and R. Hariri, "Modulation of Cell Attachment , Proliferation , and Angiogenesis by Decellularized , Dehydrated Human Amniotic Membrane in In Vitro Models," *Wounds*, vol. Epub, pp. 2–7, 2016.

[29] S. Kern, H. Eichler, J. Stoeve, H. Klüter, and K. Bieback, "Comparative analysis of mesenchymal stem cells from bone marrow, umbilical cord blood, or adipose tissue.," *Stem Cells*, vol. 24, no. 5, pp. 1294–301, May 2006.

[30] K. Bieback, S. Kern, H. Klüter, and H. Eichler, "Critical parameters for the isolation of mesenchymal stem cells from umbilical cord blood.," *Stem Cells*, vol. 22, no. 4, pp. 625–34, Jan. 2004.

[31] A. A. Rzhaninova, S. N. Gornostaeva, and D. V Goldshtein, "Isolation and phenotypical characterization of mesenchymal stem cells from human fetal thymus.," *Cell Technol. Biol. Med.*, vol. 139, no. 1, pp. 134–40, 2005.

Mary Ann Liebert, Inc.,140 Huguenot Street, New Rochelle, NY 10801

For Peer Review ONLY / Not for Distribution

[32] D. Iacobazzi, M. M. Swim, A. Albertario, M. Caputo, and M. T. Ghorbel, "Thymus-Derived Mesenchymal Stem Cells for Tissue Engineering Clinical-Grade Cardiovascular Grafts," *Tissue Eng. Part A*, p. ten.tea.2017.0290, 2017.

[33] M. F. Pittenger, A. M. MacKay, S. C. Beck, R. K. Jaiswal, R. Douglas, J. D. Mosca, M. A. Moorman, D. W. Simonetti, S. Craig, and D. R. Marshak, "Multilineage Potential of Adult Human Mesenchymal Stem Cells," *Science (80-.).*, vol. 284, no. 5411, pp. 143–147, Apr. 1999.

[34] M. Krampera, S. Sartoris, F. Liotta, A. Pasini, R. Angeli, L. Cosmi, A. Andreini, F. Mosna, B. Bonetti, E. Rebellato, M. Grazia Testi, F. Frosali, G. Pizzolo, G. Tridente, E. Maggi, S. Romagnani, and F. Annunziato, "Immune Regulation by Mesenchymal Stem Cells Derived from Adult Spleen and Thymus," *Stem Cells Dev.*, vol. 16, no. 5, pp. 797–810, 2007.

[35] C. Gonzales and T. Pedrazzini, "Progenitor cell therapy for heart disease.," *Exp. Cell Res.*, vol. 315, no. 18, pp. 3077–85, Nov. 2009.

[36] L. A. DiDomenico, D. P. Orgill, R. D. Galiano, T. E. Serena, M. J. Carter, J. P. Kaufman, N. J. Young, and C. M. Zelen, "Aseptically Processed Placental Membrane Improves Healing of Diabetic Foot Ulcerations: Prospective, Randomized Clinical Trial," *Plast. Reconstr. Surg. Glob. Open*, vol. 4, no. 10, p. e1095, 2016.

[37] E. P. Miranda and A. Friedman, "Dehydrated Human Amnion / Chorion Grafts May Accelerate the Healing of Ulcers on Free Flaps in Patients With Venous Insufficiency and / or Lymphedema," *Eplasty*, vol. 16, pp. 224–228, 2016.

[38] T. Go, P. Jungebluth, S. Baiguero, A. Asnaghi, J. Martorell, H. Ostertag, S. Mantero, M. Birchall, A. Bader, and P. Macchiarini, "Both epithelial cells and mesenchymal stem cell-derived chondrocytes contribute to the survival of tissue-engineered airway transplants in pigs.," *J.*

For Peer Review ONLY // Not for Distribution

Thorac. Cardiovasc. Surg., vol. 139, no. 2, pp. 437–43, Feb. 2010.

[39] R. L. Knight, H. E. Wilcox, S. a Korossis, J. Fisher, and E. Ingham, "The use of acellular matrices for the tissue engineering of cardiac valves," *Proc. Inst. Mech. Eng. Part H J. Eng. Med.*, vol. 222, no. 1, pp. 129–143, Jan. 2008.

[40] F. G. Scholl, M. M. Boucek, K.-C. Chan, L. Valdes-Cruz, and R. Perryman, "Preliminary experience with cardiac reconstruction using decellularized porcine extracellular matrix scaffold: human applications in congenital heart disease.," *World J. Pediatr. Congenit. Heart Surg.*, vol. 1, no. 1, pp. 132–6, Apr. 2010.

[41] M.-T. Kasimir, E. Rieder, G. Seebacher, E. Wolner, G. Weigel, and P. Simon, "Presence and elimination of the xenoantigen gal (alpha1, 3) gal in tissue-engineered heart valves.," *Tissue Eng.*, vol. 11, no. 7–8, pp. 1274–1280, 2005.

[42] MiMedx®, "EpiFix® Overview," 2017. [Online]. Available: https://www.mimedx.com/content/epifix®-overview.

[43] A. Cargnoni, M. Di Marcello, M. Campagnol, C. Nassuato, A. Albertini, and O. Parolini, "Amniotic membrane patching promotes ischemic rat heart repair," *Cell Transplant.*, vol. 18, no. 10–11, pp. 1147–1159, 2009.

[44] S.-P. Wilshaw, J. N. Kearney, J. Fisher, and E. Ingham, "Production of an Acellular Amniotic Membrane Matrix for Use in Tissue Engineering," *Tissue Eng.*, vol. 12, no. 8, pp. 2117–2129, 2006.

[45] S.-W. Cho, S. H. Lim, I.-K. Kim, Y. S. Hong, S.-S. Kim, K. J. Yoo, H.-Y. Park, Y. Jang, B. C. Chang, C. Y. Choi, K.-C. Hwang, and B.-S. Kim, "Small-diameter blood vessels engineered with bone marrow-derived cells," *Ann. Surg.*, vol. 241, no. 3, pp. 506–15, 2005.

Mary Ann Liebert, Inc.,140 Huguenot Street, New Rochelle, NY 10801

For Peer Review ONLY/Not for Distribution

[46] C. Best, S. Tara, M. Wiet, J. Reinhardt, V. Pepper, M. Ball, T. Yi, T. Shinoka, and C. Breuer, "Deconstructing the Tissue Engineered Vascular Graft: Evaluating Scaffold Pre-Wetting, Conditioned Media Incubation, and Determining the Optimal Mononuclear Cell Source," *ACS Biomater. Sci. Eng.*, no. 614, p. acsbiomaterials.6b00123, 2016.

For Peer Review ONLY/ Not for Distribution

Contact information of authors

Megan M Swim[§] (mswim90@gmail.com; 00441173422208)

Ambra Albertario[§] (aa13662@bristol.ac.uk; 00441173422208)

Dominga Iacobazzi[§] (mdxdi@bristol.ac.uk; 00441173422208)

Massimo Caputo[§] (m.caputo@bristol.ac.uk; 00441173424593)

Mohamed T Ghorbel[§] (m.ghorbel@bristol.ac.uk; 00441173424593)

[§] Bristol Heart Institute, Bristol Medical School, University of Bristol, Research Level 7, Bristol Royal Infirmary, Marlborough Street, BS2 8HW, Bristol, UK

For Peer Review ONLY / Not for Distribution

For Peer Review ONLY / Not for Distribution

FIGURE LEGENDS

Figure 1. MSCs seeded on native human amnion do not survive on the nonviable epithelial cell layer. (**a**) Human amnion (AM) dissected from the fetal side of the placenta and PBS washed. (**b**) Surface morphology of control amnion using scanning electron microscopy (representative images, n=4, bar=100 μm). (**c**) H&E and (**d**) EVG stained amnion showing a layer of native epithelial cells (black arrows) on the surface with a collagen (white arrows) matrix ~~(bar 50=μm)~~ (representative images, n=4, bar=50μm ~~12 samples collected~~). (**e**) Viability testing showed dead epithelial cells (Ethidium III, red) and only one viable cell (Calcein, green) (Hoerscht, blue) (representative images, n=4, bar=50 μm). (**f**) SEM indicated the epithelial cells were damaged as the cobblestone morphology was altered. There were no visible seeded MSCs (representative images, n=4, scale bar=100 μm). (**g**) Representative image of epithelial cells still visible on the surface of the H&E staining with no additional nuclei ~~or proliferation~~ (representative images, n=4, bar=50 μm). (**h**) EVG demonstrates AM's ~~that no new~~ collagens contents ~~are produced~~ (representative images, n=4, bar=50 μm).

Figure 2. **(a)** Cell viability, H&E, EVG and SEM of decellularized AM and decellularized AM-seeded with T-MSCs. Ethidium and calcein viability stain shows no residual live or dead epithelial cells visible after decellularization. Viability staining shows MSCs seeded on the surface of the decellularized amnion are sparse but viable (representative images, n=5, bars=50 μm). H&E and EVG of the decellularized AM demonstrates no remaining nuclear material or damage to collagens following decellularization (representative images, n=5, bars=50 μm). H&E of the decellularized AM-seeded with T-MSCs shows a thin layer of cells on the surface of the

Mary Ann Liebert, Inc.,140 Huguenot Street, New Rochelle, NY 10801

decellularized AM (black arrows). EVG of the same material shows intact collagens (white arrows). SEM shows the fibers on the surface of the decellularized AM without epithelial cells. SEM of the decellularized AM-seeded with T-MSCs shows cells covering the decellularized AM fibers (representative images, n=5, bars=100 μm).

(b) Macroscopic view, H&E, EVG and SEM of decellularized single-layered dried AM and decellularized multi-layered dried AM. The macroscopic view shows images of the single-layered and multi-layered decellularized AM dried for preservation. Cross sections of H&E show no residual nuclear material on both single and multi-layered materials. H&E also shows one layer of AM in the single-layered material and four layers of AM in the multi-layered construct (representative images, n=5, bars=50 μm). EVG staining shows a compact set of collagens with no damage in the single- and multi-layered materials (representative images, n=5, bars=50 μm). SEM demonstrates the decellularized surface topography of the single- and multi-layered materials (representative images, n=5, bar=100 μm).

(c) Cell viability, H&E, EVG and SEM of decellularized single- and multi-layered dried AM (d-AM-fd-single, d-AM-fd-multi) seeded with T-MSCs. Live/dead staining demonstrates mainly viable cells on the surface of d-AM-fd-single seeded and d-AM-fd-multi-seeded (representative images, n=5, bars=50 μm). Cross sections of H&E show a thin layer of cells on the surface of the d-AM-fd-single seeded (black arrows) and a thicker layer of cells on the surface of the d-AM-fd-multi-seeded (black arrows, representative images, n=5, bars=50 μm). EVG staining shows the compact set of collagens with some loose collagens in the single- and multi-layered materials. The loose collagens could possibly be newly formed by the seeded cells (white arrows, representative images, n=5, bars=50 μm). SEM shows the topography of the seeded cells on the

For Peer Review ONLY - Not for Distribution

surface of d-AM-fd-single-seeded and d-AM-fd-multi-seeded (representative images, n=5, bars=100 μm).

Figure 3. Quantification of improved cell viability on the surface of dried decellularized matrix. Cell viability staining indicated that the dried native amnion (**a**, AM-fd-seeded) seeded with cells on the surface had very few viable cells while the dried decellularized matrix (**b**, d-AM-fd-single-seeded) and multilayered decellularized dried matrix (**c**, d-AM-fd-multi-seeded) seeded with cells exhibited more viable cells (bars=50μm). (**d**) Quantification of MSC survival on the AM-fd-seeded versus the d-AM-fd-single-seeded ($p=0.023$) and d-AM-fd-multi-seeded ($p<0.001$) shows significantly higher cell survival on the surface of the decellularized freeze-dried tissue (AM-fd-seeded n= 6, d-AM-fd-single-seeded n=3, d-AM-fd-multi-seeded n=7; all technical triplicate).

Figure 4. Ultimate tensile strength and Young's Modulus of the amnion. Native (AM, n=4), decellularized (d-AM, n=4), single layer decellularized dried and seeded (d-AM-fd-single, n=4; d-AM-fd-single-seeded, n=4, respectively), multi-layered decellularized dried (d-AM-fd-multi, n=4) and d-AM-fd-multi-seeded (n=4) cultured for 7 days were compared for ultimate tensile strength ~~tensile stress at maximum load~~ and Young's Modulus. (**a**) The d-AM-fd-multi and d-AM-fd-multi-seeded were significantly stronger than the AM ($p < 0.0001$; $p = 0.004$), the d-AM ($p < 0.0001$; $p = 0.011$), the d-AM-fd-single ($p < 0.0001$; $p = 0.021$), and the d-AM-fd-single-seeded ($p < 0.0001$; $p = 0.0126$) respectively. There was no significant difference between the unseeded d-AM-fd-multi and d-AM-fd-multi-seeded ($p = 0.96$). (**b**) d-AM-fd-multi was

For Peer Review ONLY // Not for Distribution

significantly less ~~more~~ elastic than the AM ($p < 0.0001$), dAM ($p = 0.00044$), d-AM-fd-signle ($p = 0.00077$), and d-AM-fd-single seeded ($p = 0.0033$).

Figure 5. d-AM-fd-multi was able to support the cell growth of different ~~multiple~~ cell types suitable for cardiovascular tissue engineering. Human umbilical cord blood mesenchymal stem cells (**a**, hUCB-MSCs), human umbilical vein endothelial cells (**a**, hUVECs), human umbilical artery smooth muscle cells (**b**), and cardiac myocytes (**b**) were all able to adhere and survive on the surface of the d-AM-fd-multi. A layer of cells (black arrows) was visible on the surface of the matrix as demonstrated by H&E **(a, b)**. EVG (**a, b**) staining shows a compact set of collagens with some loose collagens (white arrows) that could possibly be newly formed by the seeded cells (representative images, n=4, bars=50 μm) ~~and (c, g, k, o) began to produce their own extracellular matrix (white arrows) (bars=50 um)~~. SEM (**a, b**) shows the topography of the seeded cells on the surface of d-AM-fd-multi ~~Surface morphology showed that all cell types were adhering to the matrix~~ (representative images, n=4, bars=100 μm).

Figure 6. d-AM-fd-multi implanted into the pig model produced a viable graft. (**a**) d-AM-fd-multi was implanted into the left pulmonary artery (LPA) of the piglet model. (**b**) Image of the implanted graft. ~~Graft supported blood flow after implantation in the left pulmonary artery~~. (**c**) Following 2.5 months in vivo, explanted graft had integrated within the surrounding tissue. (**d**) Patent ~~Blood flowed through the~~ LPA with normal blood velocity shown by echocardiograms and Dopplers at the time of surgery, immediately post-surgery, and 2.5 months after surgery. (**e**) H&E and EVG of explanted graft compared to native left pulmonary artery demonstrate

For Peer Review ONLY - Not for Distribution

extensive nucleation ~~cell infiltrate~~ and collagen production (representative images, n=2, bars=1000 μm). (**f**) Cross sections H&E of graft away from suture, graft close to suture and native left pulmonary artery (representative images, n=2, bars=50μm).

(**g**) The native left pulmonary artery and implanted graft show a similar endothelial lining on the surface of the inner side indicated by SEM (bars=100μm). (**h**) Fluorescent staining of the graft cross sections ~~Immunohistochemistry~~ indicates that the cells on the inner side are endothelial cells (iso, green). It also shows smooth muscle cell markers (aSMA, smMYH and CNN in red, red and green respectively) throughout the media ~~(aSMA (red), smMYH (red), and CNN(green))~~ (representative images, n=2, bars= 50μm). (**i**) Cross sections of H&E (bar=50μm) and fluorescent staining (bar=100μm) of the graft adventitia showing the vasa vasorum (representative images, n=2).

~~**Supplementary Figure 1.** Morphology and characterization of cardiac myocytes, hUVECs, and smooth muscle cells. Cardiac myocytes from Promo Cell were stained with cardiac markers, Conn 43 and Desmin and were positive for both (red). hUVECs were stained for endothelial markers VWF (green) and CD31 (red) and were positive for both. Smooth muscle cells were stained for smooth muscle markers SMA (green), calponin (green) and myosin heavy chain (red) and were positive for all three (bars=50 um).~~

For Peer Review ONLY // Not for Distribution

Figure 1

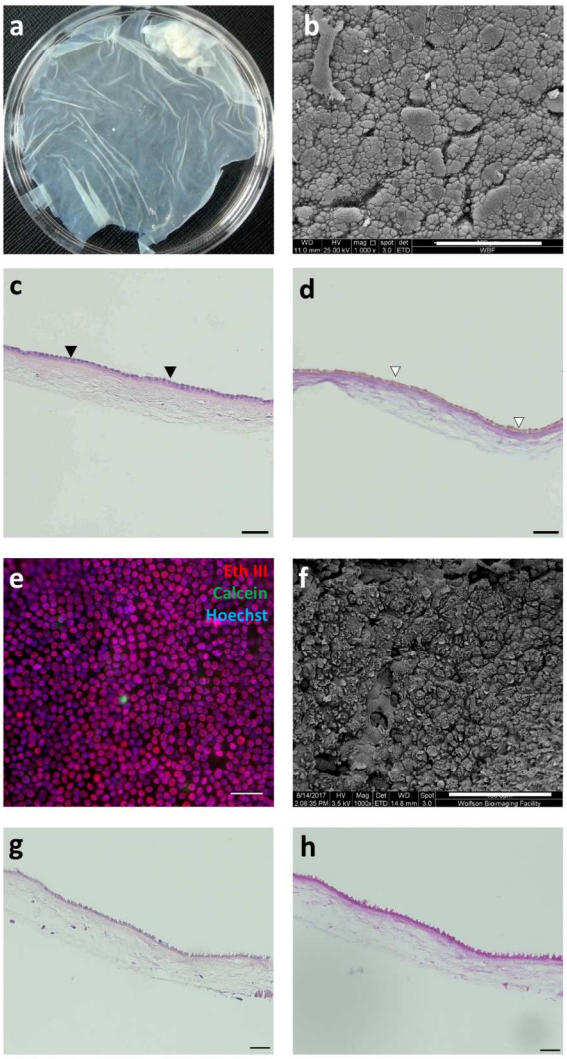

Fig1

586x846mm (72 x 72 DPI)

Figure 2

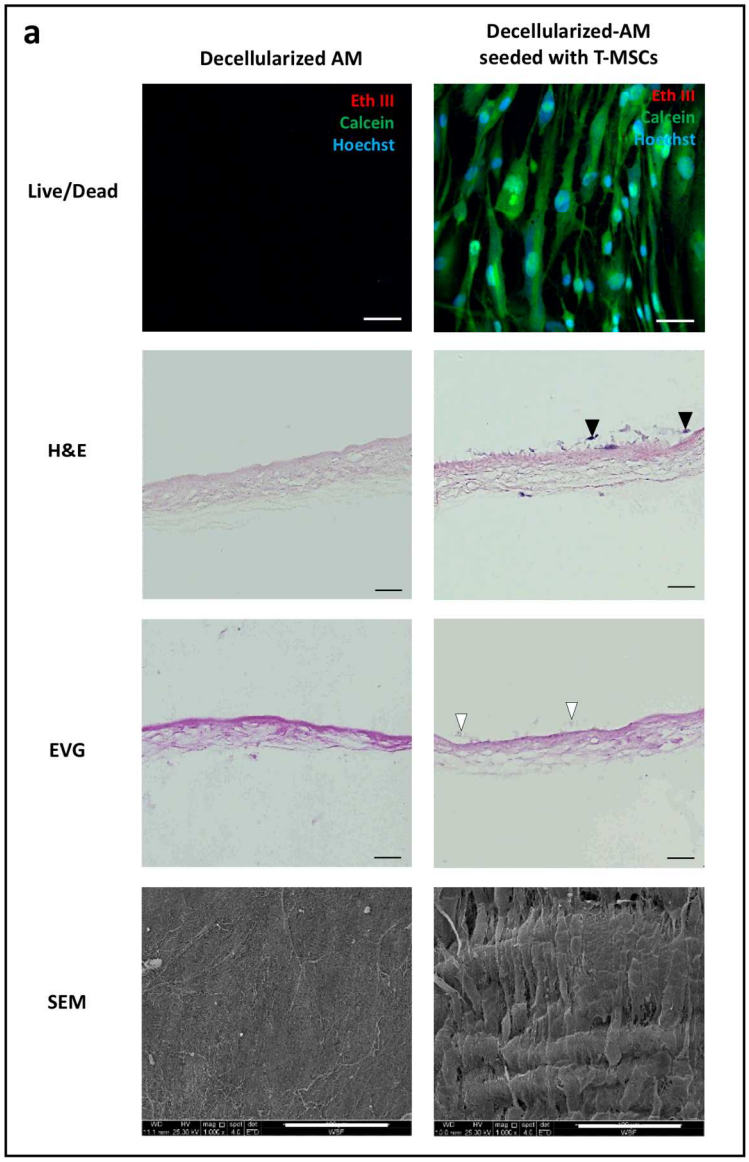

Fig2a

586x846mm (72 x 72 DPI)

Figure 2

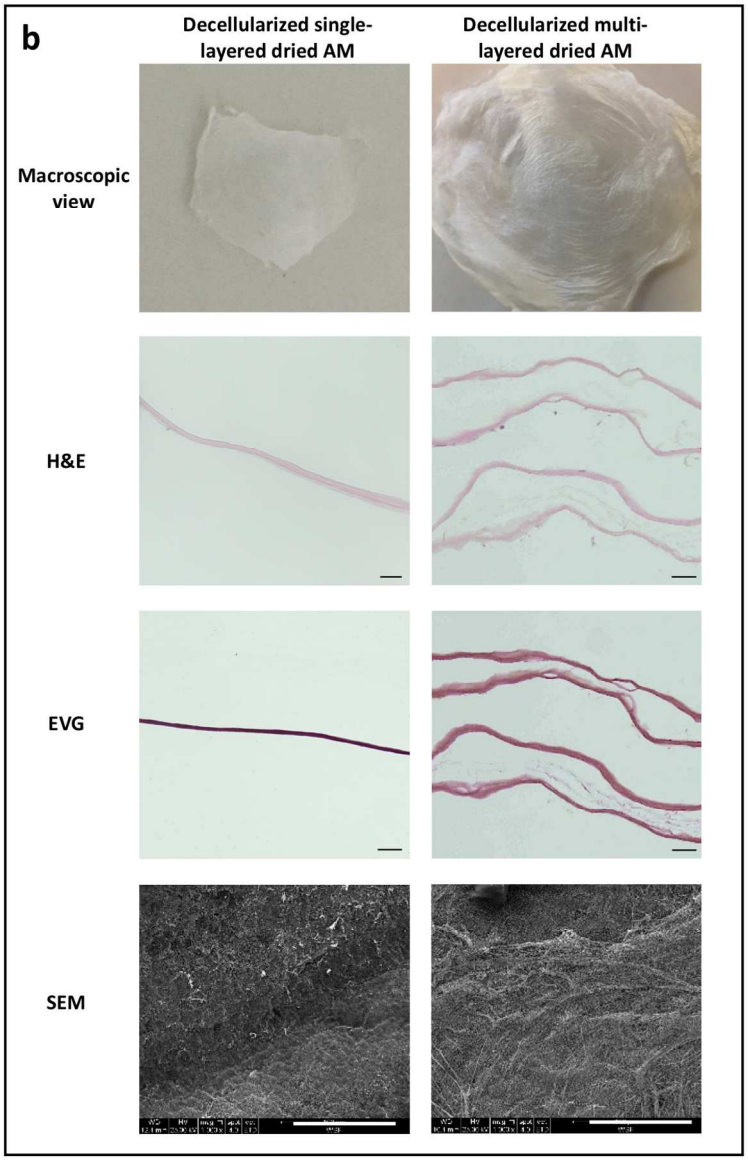

Fig2b

586x846mm (72 x 72 DPI)

Figure 2

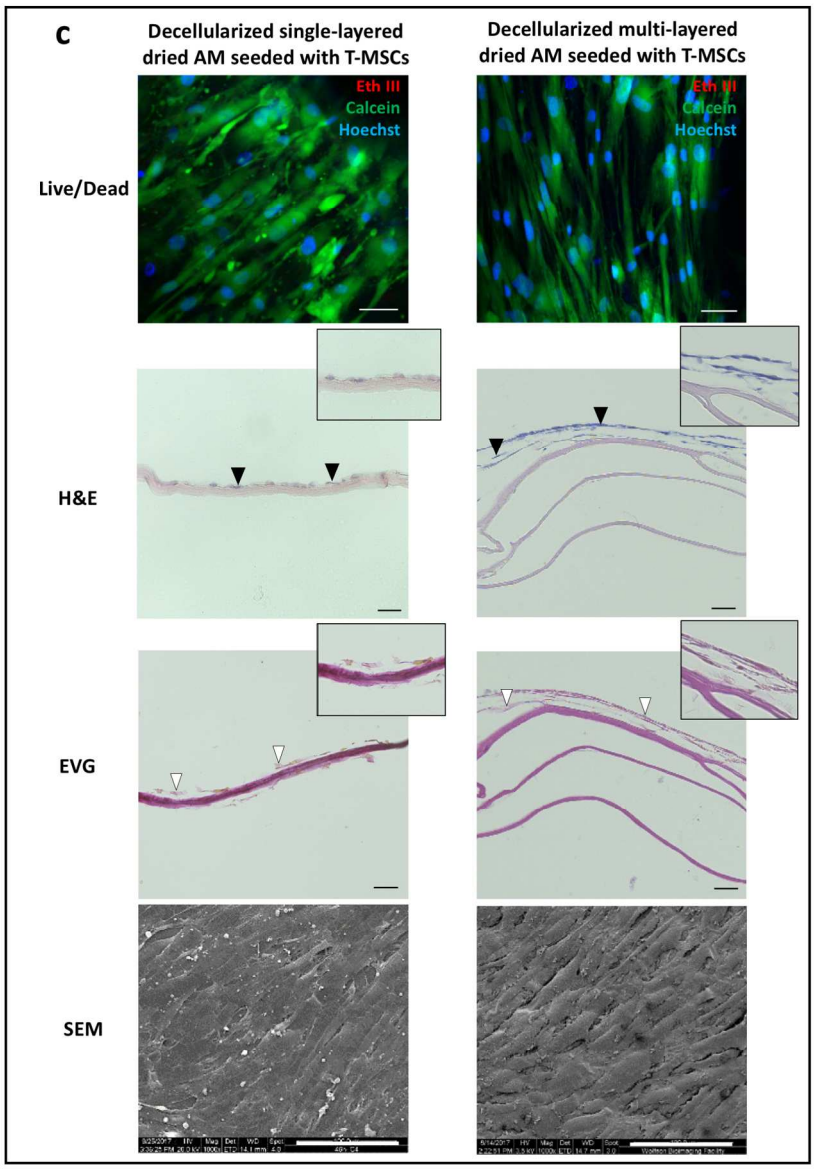

Fig2c

586x846mm (72 x 72 DPI)

Figure 3

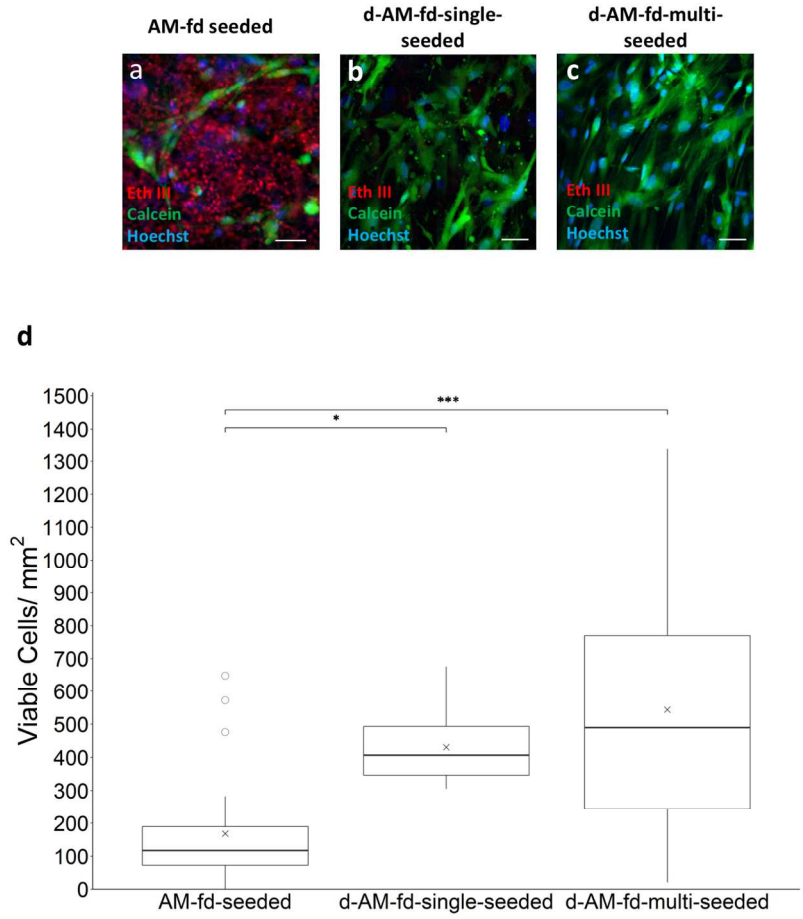

Fig3

586x846mm (72 x 72 DPI)

Figure 4

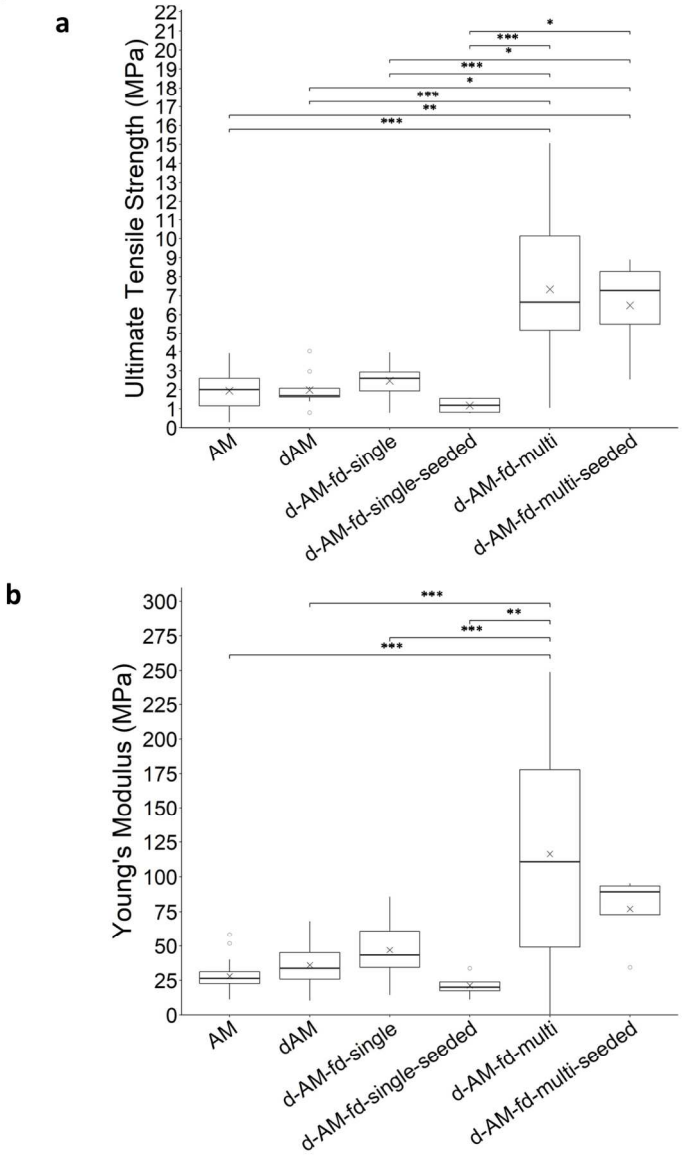

Fig4

586x846mm (72 x 72 DPI)

Figure 5

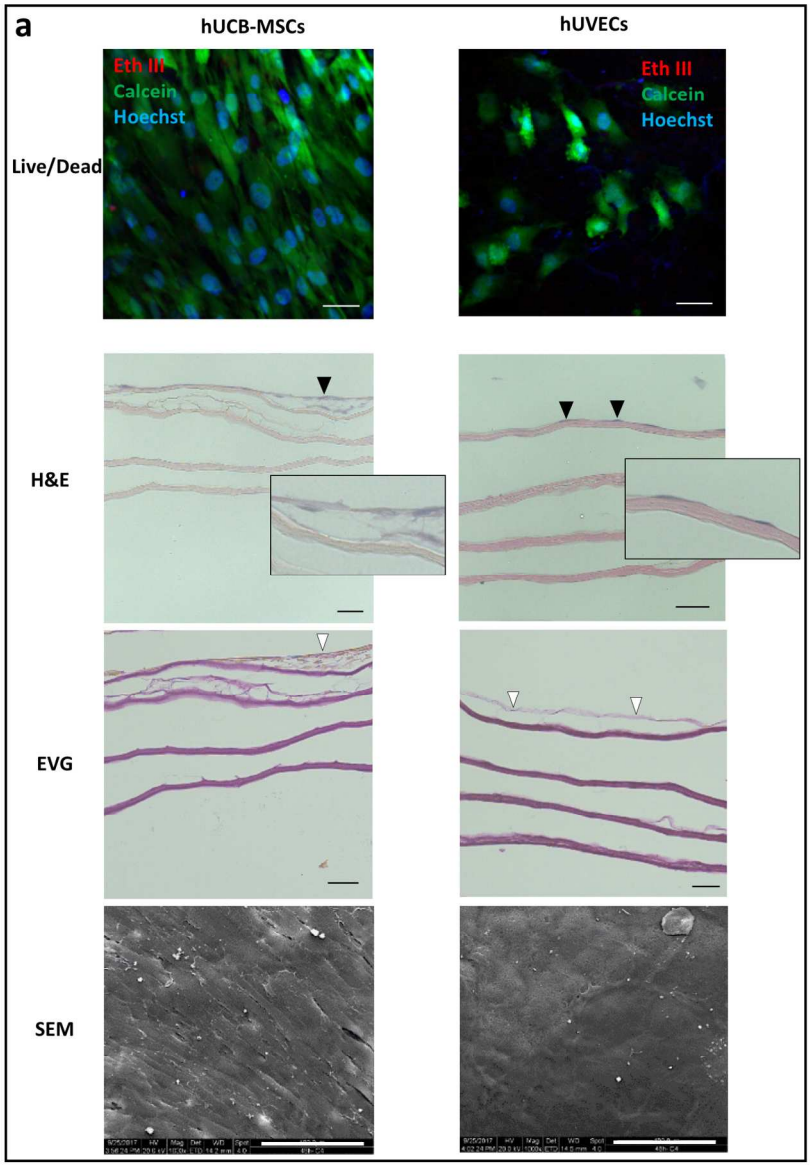

Fig5a

586x846mm (72 x 72 DPI)

Figure 5

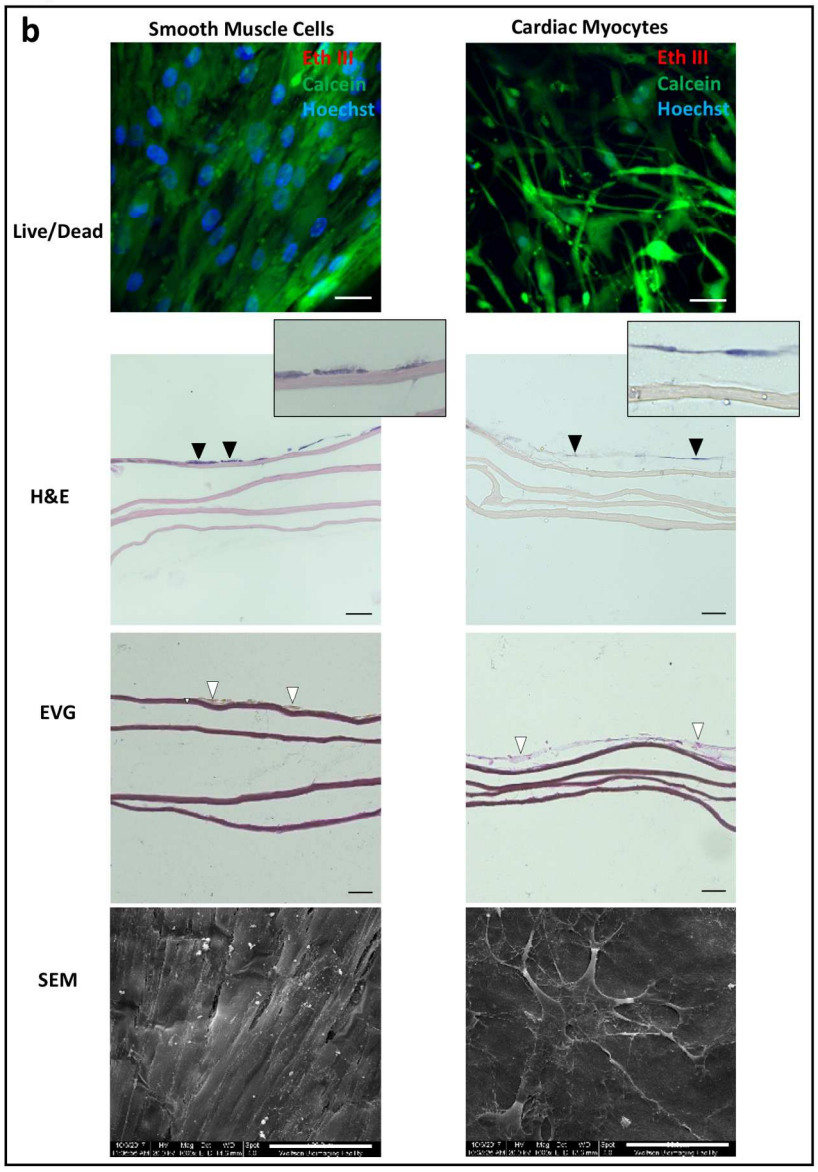

Fig5b

586x846mm (72 x 72 DPI)

Figure 6

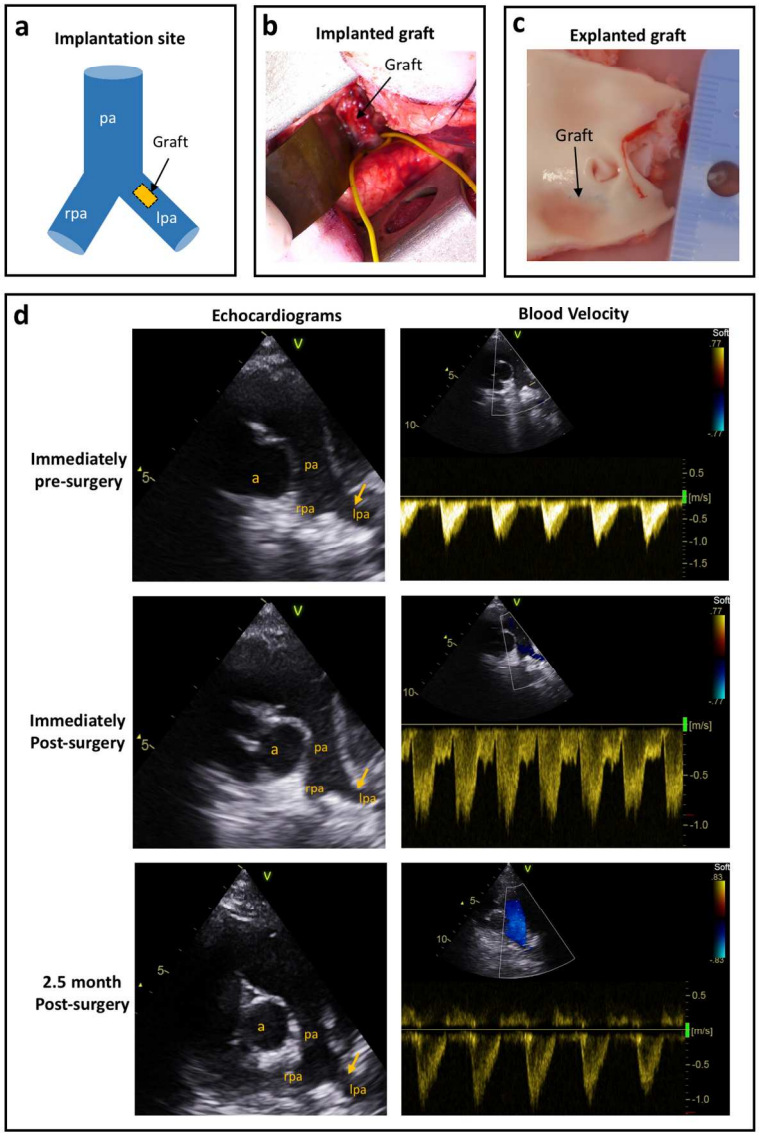

Fig6a-d

586x846mm (72 x 72 DPI)

Figure 6

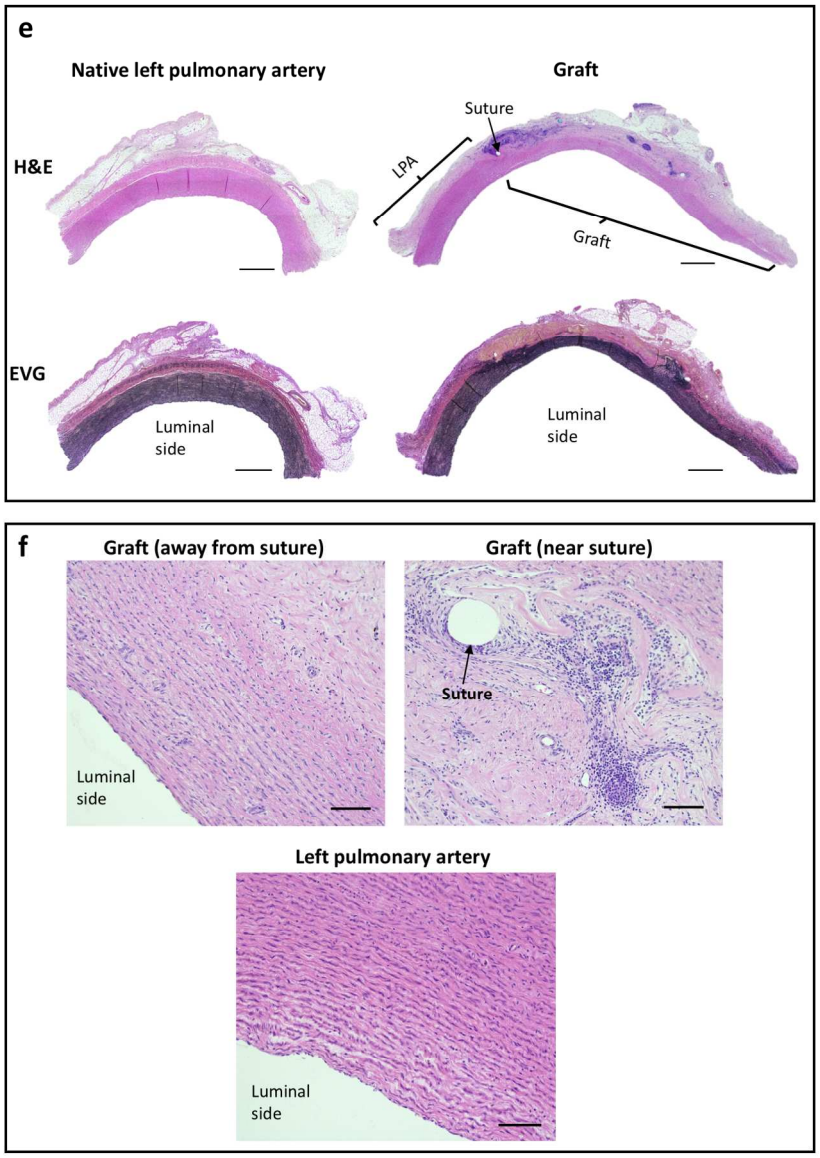

Fig6e-f

586x846mm (72 x 72 DPI)

Figure 6

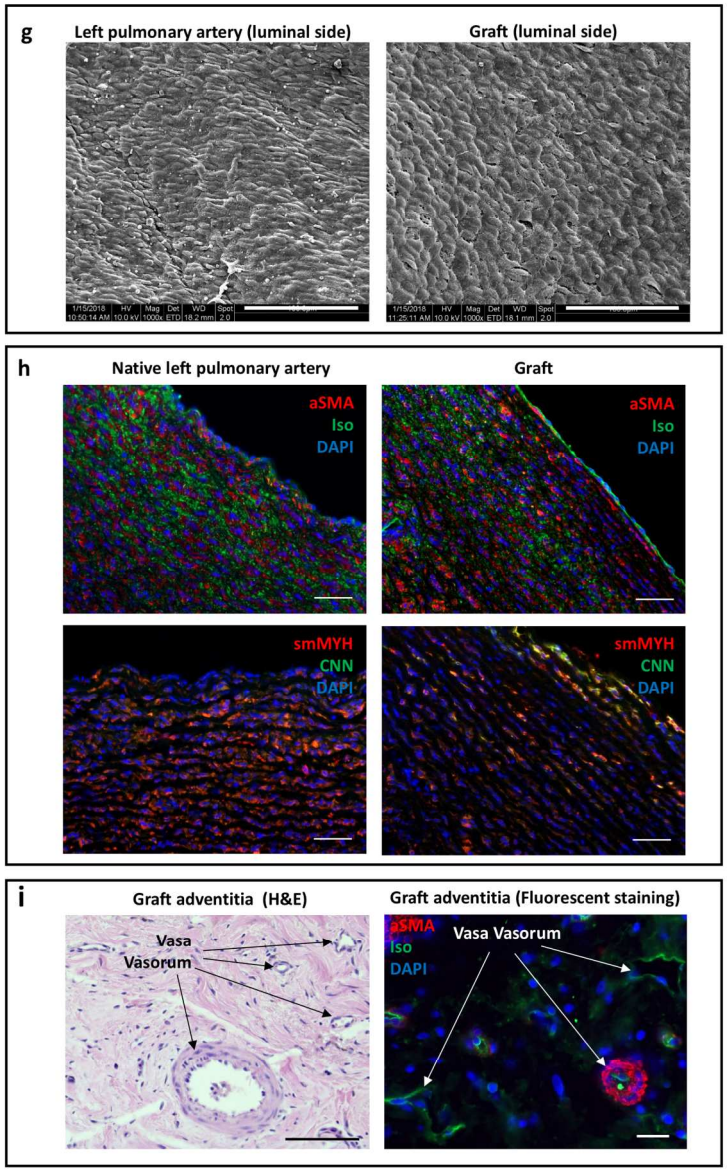

Fig6g-i

586x846mm (72 x 72 DPI)